Journal of Applied Polymer Science

Miscible raw lignin/nylon 6 blends: Thermal and mechanical performances

Naïma Sallem-Idrissi,[1] Michel Sclavons,[1] Damien P Debecker,[2] Jacques Devaux[1]

[1]Bio-and Soft Matter (BSMA), Institute of Condensed Matter and Nanosciences (IMCN), Université Catholique De Louvain (UCL), Croix Du Sud 1, Box L7.04.02, Louvain-la-Neuve, B-1348, Belgium

[2]Molecules, Solids and Reactivity (MOST), Institute of Condensed Matter and Nanosciences (IMCN), Université Catholique De Louvain (UCL), Croix Du Sud 2, Box L7.05.17, Louvain-la-Neuve, B-1348, Belgium

Correspondence to: N. Sallem-Idrissi (E-mail: naima.sallem@uclouvain.be)

ABSTRACT: Environmentally friendly bio-filled composites of various proportions of polyamide 6 (PA6) and technical lignin have been prepared using a twin-screw extruder. Transmission electron microscopy has been used to investigate the morphology of the composites. It reveals homogeneous single phase system, indicating the miscibility of PA6 and lignin. The glass transition temperature of the blends, determined by DMA, was shifted systematically to higher temperature with increasing concentration of lignin which highlights the miscibility of both components. In addition, Fourier Transform Infrared analyses have shown that new specific hydrogen-bonding interactions are formed between hydroxyl groups of lignin and amine groups of the PA6. The presence of these intermolecular interactions between PA6 and lignin strongly influenced the thermal stability of the blends by lowering the onset of the blend's degradation process. However, the blends exhibit good mechanical properties whatever the lignin content. © 2015 Wiley Periodicals, Inc. J. Appl. Polym. Sci. **2016**, *133*, 42963.

KEYWORDS: cellulose and other wood products; extrusion; polyamides

Received 12 May 2015; accepted 16 September 2015

DOI: 10.1002/app.42963

INTRODUCTION

The development of environmentally friendly materials, has led to a growing interest in biofiller polymer composites research activity. To this end, natural and organic polymers such as lignin and cellulose fibers, have been selected because they offer a number of advantages compared with synthetic materials such as being biodegradable, CO_2 neutral, available abundantly. Furthermore, agricultural nonfood commercial residues could be used as a source of raw, renewable, and inexpensive materials for the plastic industries.[1] Lignin is one of the major components of wood along with cellulose and hemicellulose. It is a large source of organic raw material, about 4–35% of most biomass, 16–25% of hardwoods, and 23–35% of softwoods.[2–4] Despite being frequently used as a low-cost fuel for the internal energy needs of paper plant and biorefineries, large quantities of lignin are available in these industrial sectors and more value-added application is sought for.[5–7] Because of its very complex structure, a small fraction is used for relatively low-value and limited applications such as concrete additives, dyestuff dispersants, binders or surfactant for animal feed, dust control, and pesticides.[3,8,9]

Indeed, lignin is described as a complex amorphous aromatic polymer characterized by a highly branched three-dimensional phenolic structure including three main phenylpropane units, namely p-coumaryl, coniferyl, and sinapyl. The resulting phenolic substructures are called p-hydroxyphenyl (H, for coumaryl alcohol), guaiacyl (G, for coniferyl alcohol), and syringyl (S, for sinapyl alcohol) moieties. The monolignols units are linked together via radical coupling reactions and consist of almost 50–60% β-O-4 ether linkages.[10,11] Moreover, lignin composition and content are influenced by a number of factors like botanical origin, environmental conditions of growth, and the extraction processes.[7] For example, hardwood lignins consist mainly of G and S units and traces of H units, whereas softwood lignins are mostly composed of G units, with low levels of H units.[12–15] Based on the first full lignin structure proposed by Adler in 1977, lignin is recognized as a highly branched polymer with a variety of functional groups: aliphatic and phenolic hydroxyls, carboxylic, carbonyl, and methoxyl groups.[15] Most efforts to utilize lignin have been limited by various factors that impart in its characteristics defining it as an unreliable precursor to polymer production. Lignin and more specifically technical lignin indeed offer relatively unpredictable polymerization characteristics, depending

upon their source and the degree of delignification to which the plant materials were submitted. More specifically, the highly functional character of lignin induces a variety of potential polymerization sites and causes heat instability in such materials. However, the presence of numerous possible reaction sites makes lignin convenient for chemical modifications, and grafting sites. Hence, despite structural disadvantages, lignin appears as a prospective candidate for being a component of value-added products in new applications. Recently a significant potential for a greener carbon fiber production has been reported using lignin blended with bio or oil-based polymers.[16–21] Lignin was also used as coupling agent in thermoplastic and rubbers in order to promote the affinity between constituents and/or to improve the mechanical properties of the matrix as reported in recent works.[22,23] During the last decades, various scientific and technological researches devoted to the synthesis and the characterization of lignin-containing polymers confirm this enthusiasm.[24–30]

The main uses of lignin can be classified into two different groups: (1) without chemical modification where lignin is directly incorporated into a polymer matrix to give new or improved properties, and (2) with chemical modification to prepare a large range of chemicals, building blocks and polymers. One of the possible and economic applications for lignin is its blending with polymeric materials to increase their content of renewable, cheap resources and to develop new polymer materials. However, raw lignin's incorporation in solid material system is hindered by its extensive cross-linking and strong intermolecular interactions. As a consequence raw lignin is a rarely miscible with most synthetic polymers and mainly negative effects are observed on the mechanical properties. The elongation at break is generally drastically decreased by lack of cohesion while the tensile strength can barely be maintained constant.[13,31] Through polymer blending these interactions could be disrupted, thus altering the lignin's melt flow characteristics. This reduction of the degree of self-association between lignin molecules must improve lignin–polymer miscibility. Chemical derivatization of lignin could also help but with the drawback to cancel the environmental and economic advantage of using such bio-based resource.[14,32,33]

The most usual way to produce new polymer materials is by melt-blending in an extruder because it is inexpensive, environmentally friendly, and straightforward. By this way, direct incorporation of raw lignin into polymer materials like poly(ethylene terephthalate) (PET), poly(vinyl alcohol) with different hydroxyl concentration, poly(ethylene oxide) (PEO), poly(vinyl chloride), polypropylene, polyethylene, polystyrene, poly(hydroxybutyrate) (PHB), poly(lactid acid) (PLA), and many others, have been already reported.[17,20,29,31,34–50]

However, it is generally difficult to prepare miscible blends owing to the low entropic benefit of mixing and to its endothermic character because of a significant absence of intermolecular interactions resulting in phase-separated systems. Therefore, in most cases, to reach miscibility or practically good compatibility, some attractive intermolecular interactions between the component polymers should be found. Recently, some works have been devoted to the intermolecular interactions to obtain lignin-based polymer blends, for example, an ionic interaction hydrogen bonding attraction, and a specific structure of the counterpart polymer were looked for to improve the miscibility or compatibility of two constituent polymers.[32,47,49,50] Miscible blends of lignins were observed only with PEO, PET, PHB, PVC, and Poly(N-vinyl pyrrolidone) (PVP).[34–36,38–42,49,51] The glass transition (T_g) of these blends showed a negative deviation from a linear mixing rule, indicative of specific intermolecular interactions. Infrared analysis revealed the formation of a strong intermolecular hydrogen bonds between the hydroxyl aromatic proton of lignin and the ether oxygen of PEO structure.[13,17,38,39] Identical analytical observations have been made for the PET and PHB.[36,49]

The main goal of this article is to demonstrate the possible use of raw lignin powder as a filler for polyamide and especially for polyamide 6 (PA6) matrix. To the best of our knowledge, blends of lignin and polyamide have been examined only once with PA11.[48] No report has been found on PA6 blended with lignin by direct extrusion technology without any chemical pre or in-situ modifications or physical pretreatments and where the presence of various organic and inorganic impurities in the selected technical lignin have been maintained. Here, the incorporation of this cheap renewable material from biomass in PA6 is inspected by an array of characterization tools. Also, the effect of the presence of lignin on the morphology and on the properties of the resulting materials is investigated.

Differential scanning calorimetry (DSC), dynamic mechanical analysis (DMA), Fourier Transform infrared spectroscopy (FTIR), mechanical testing, and transmission electron microscopy (TEM) analyses have all revealed the miscibility of PA6 and lignin. For example, the glass transition temperature T_g is found to shift in case of blend formation indicating strong intermolecular interactions. FTIR analyses have further evidenced that new specific hydrogen-bonding interactions are formed between hydroxyl groups of lignin and amine groups of the PA6. The presence of these intermolecular interactions between PA6 and lignin seems to lead to an enhancement of the blends ductility. Especially, the blends exhibit good mechanical properties whatever the lignin content.

EXPERIMENTAL

Materials

The blends were carried out with commercial soda pulp lignin from agricultural residues (Protobind 1000 by ALM India, Chandigarh 160009, India; Mn = 65,000 g mol^{-1}, T_g = 102°C). Lignin was used as received and was not dried before extrusion. The matrix used was an extrusion grade polyamide 6 (PA6) (grade Durethan B40 F) from LANXESS. Its intrinsic viscosity is 225 cm^3/g (ISO 307). Before extrusion PA6 pellets were dried in a vacuum oven at 80°C for 12 hours.

Composite Preparation

The neat PA6 and all blends (Table I) were prepared in a co-rotating twin-screw extruder Krupp WP ZSK25, with a screw length of 1000 mm and L/D ratio of 40. The extrusion process was conducted at 240°C with a screw speed of 300 rpm. PA6 and lignin were introduced in the melting zone using a

Table I. Composition of PA6/Lignin Blends

Sample	PA6 (wt %)	Lignin (wt %)
PA-L0	100	0
PA-L5	95	5
PA-L10	90	10
PA-L15	85	15
PA-L30	70	30

throughput of 7 kg/h. The residence time in the extruder was around 1.5 min. Finally, extruded samples were immediately quenched at room temperature and pelletized.

Blend pellets were then injection-molded using a Krauss-Maffei type KM 80-160E injection-molding machine in standard dog-bone specimens (ASTM 527) for tensile tests. The barrel temperatures ranged within 200–240°C and the mold temperature was kept at 25°C. Before injection, pelletized samples were dried in a vacuum oven at 25°C for two weeks and at 60°C during 12 hours just before the injection-molding.

Characterization

Structural Characterization. ***Transmission electron microscopy.*** A transmission electron microscope LEO 922 (Zeiss) with a 200 kV acceleration voltage was used to examine the dispersion state of lignin in the polyamide matrix. The specimens for TEM analysis were cut from bulk compounds and from the dog-bone specimens at room temperature using a Reichert Microtome. Ultrathin sections of approximately 90 nm thickness were cut using a cryodiamond knife with a cut angle of 35° (Diatome, Switzerland) and collected on 400 mesh copper grids.

Fourier transform infrared spectroscopy. FTIR spectra were recorded on a Nicolet Nexus 870 FTIR spectrometer on compression-molded films in transmission mode by collecting 16 scans at a resolution of 4 cm^{-1} over a spectral range from 4000 to 400 cm^{-1}. Spectra of the lignin powder were collected by using a KBr pellet. Spectra were normalized by setting the peak height of 1168 cm^{-1} absorption band to an absorbance of 1. This band, which is assigned to CH_2 twist/wag of PA6, is usually considered as an internal reference for comparison of films of different thicknesses. For comparison, the spectra were also normalized with the CH_2 band at 2860 cm^{-1} with no significant difference.

Thermal and Mechanical Characterization. ***Differential scanning calorimetry (DSC).*** DSC analyses were performed on a DSC 821e (Mettler Toledo, Switzerland). Lignin samples and blend samples of around 10 mg were subjected to a first heating ramp from 25°C to 200°C followed by a cooling ramp from 200°C to 25°C. The heating/cooling rate of each segment was 10°C/min. The role of the first heating run is usually to erase the thermal history of the sample.

Thermogravimetric analysis (TGA). Thermal stability of the references and of the blends was studied by TGA. The analyses were performed using TGA/SDTA 851e (Mettler Toledo, Switzerland). The samples ($\approx 10 \pm 0.5$ mg) were placed in open alumina crucibles of 70 µL and heated from room temperature to 1000°C at a constant rate of 20°C/min under air and nitrogen atmosphere with a flow of 100 mL/min for neat PA6 and the blends and 50 mL/min for lignin powder.

Dynamic mechanical analysis. Thermo-mechanical measurements were performed using a DMA/SDTA 861e (Mettler-Toledo, Switzerland) on rectangular specimens of dimension 2.0 × 4.0 × 9.0 mm^3 prepared by injection-molding. The measurements were performed under tension at a constant frequency of 1 Hz. The maximum force was 3 N and the maximum displacement was 4 µm. Experiments were performed in a temperature range from −50°C to 150°C at a heating rate of 3°C/min. Presented results are average of three experiments.

Supported DMA: In order to highlight the lignin thermal transitions, supported DMA was performed on lignin powder sandwiched between rigid copper foils (of dimension 8 × 0.3 × 70 mm^3) and the whole was packed by an aluminum sheet to avoid any lignin losses. This technique has been already used to assess thermal properties of coatings and nanocoatings by Carlier *et al.* and demonstrated that the less stiff material response is mainly recorded and strongly amplified.[52] Like in Carlier's work, lignin system was subjected to a dual cantilever deformation in order to favor the shear strain of the lignin. The maximum force was 1.5 N and the maximum displacement was 10 µm. The analyses were performed at a constant frequency of 1 Hz from −50°C to 200°C.

Mechanical testing. Tensile tests were performed at room temperature using a universal tensile machine (Zwick Roell Retro-Line) equipped with a 50kN load cell. All injection-molded specimens had a dog-bone shape according to the standard ISO 527-3 type V, with an average cross section of 5.7 × 2 mm^2 at the gauge length region. Tests were conducted at a crosshead speed of 1 mm/min for Young's modulus measurements. This latter was calculated from the slope of the stress–strain curve in the elastic regime (between 0.05% and 0.2% strains). The tensile yield strength and the elongation at break were measured at a loading rate of 50 mm/min. Property values reported in this work represent an average of five replicates for each sample.

RESULTS AND DISCUSSION

Morphological Characterization

All blends exhibited good thermal processing properties. Extrusion torque decreased with increasing addition of lignin from 47% for PA to 27% for a lignin addition of 30 wt %. In this last case, the extrusion temperature has been adjusted at 190°C (instead of 240°C) to improve the strand's handling. Similarly, the injection temperature was lowered (from 240°C to 190°C) to be close to extrusion temperature and to inevitably preserve the samples from degradation. This plasticizing effect indicates a change in the physical properties of the mixture or its components, such as inter-chain interactions upon changing blend composition. No change is noted when dried lignin is added. The same behavior has been already described for thermal processability of kraft and organosolv lignin/PEO blends.[13,38,39]

The efficiency of lignin for blending in the polymer matrix is primarily determined by the degree of its dispersion in the matrix. Interestingly, no aggregates of lignin are visible to the

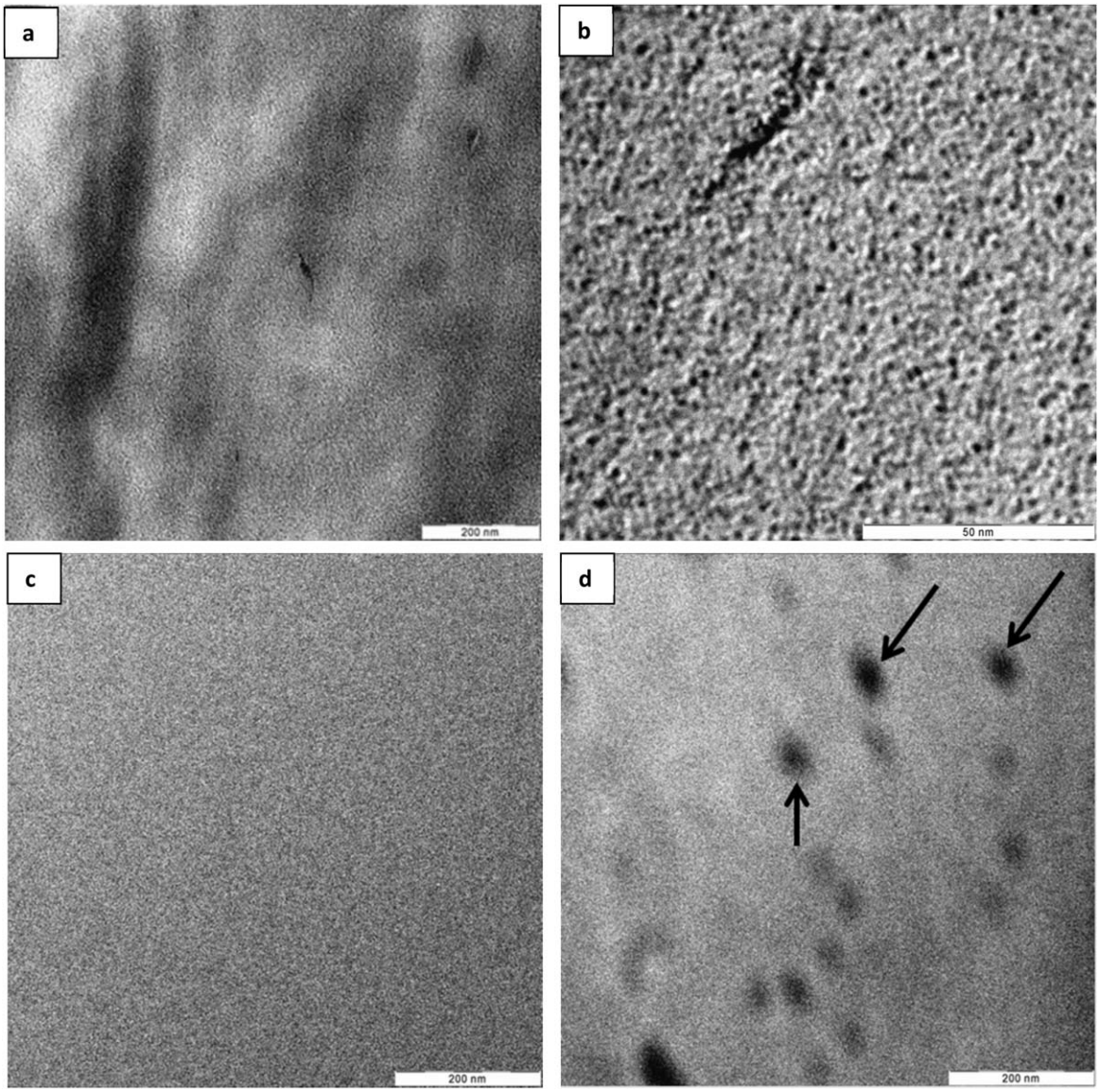

Figure 1. TEM micrographs of: (a) and (b) PA-L5, (c) PA-L15 and (d) PA-L30. Arrows indicate lignin nodules.

naked eye and by optical microscopy of extruded samples for the all studied concentration range. Moreover, the corresponding cooled strand could be stretched by hand like the pristine matrix. A better observation of the dispersion at the nanoscale was carried out by TEM observations. Figure 1 shows representative TEM views of the bulk in the different extruded samples. At this scale and in opposite to the case of PA11,[48] no trace of lignin aggregates were visible on the analyzed samples except for the highest lignin concentration where some aggregates [indicated by arrows in the picture (d)] less than 100 nm in diameter are present but well-dispersed. The grey area corresponds to the PA matrix and the darker regions are attributed to lignin inclusions. The strips preferentially observed on the picture (a) are because of the knife marks generated during cutting, whereas the presence of lignin nano-agglomerates in the 30 wt % [see Figure 1(d)] is only due in our point of view, to a lack of room for diffusion.

The same qualitative observations were made on the corresponding injected samples (not shown here). Even when subjected to heat at 240°C for 3 hours in air or N_2, injected specimens yield the same morphological images. No distinct phase-separated domain can be distinguished, ruling out possible coalescence phenomena. Up to 30 wt %, TEM observations confirm in every case the absence of aggregates and a dispersion of the selected lignin at a sub-nano level [around 1 to 2 nm as can be seen in Figure 1(b)] in PA6 matrix suggesting a stable miscibility of both components.

Thermo-Mechanical Properties

Blend miscibility is usually highlighted by the presence of a single glass transition temperature (T_g). In this way, DSC was performed to determine T_g of the blends. Owing to the intrinsic broadened transition of lignin which hides the heat capacity jump, it was however difficult to measure T_g of the blends from

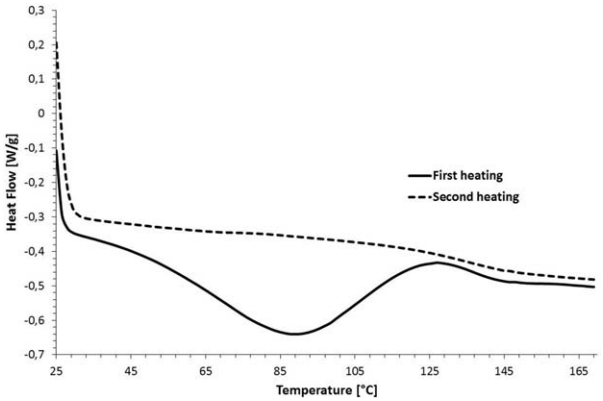

Figure 2. DSC thermograms of neat lignin.

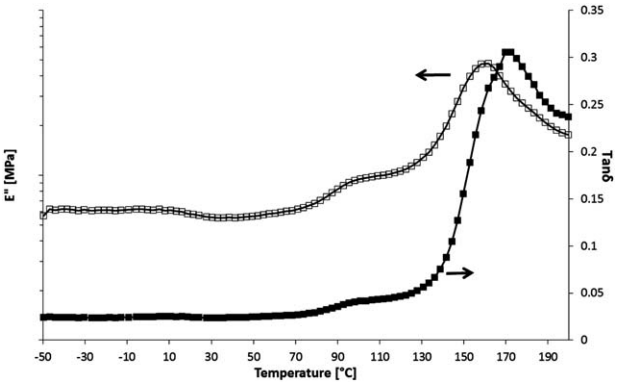

Figure 3. Loss modulus (E'') and Phase angle (Tan δ) of neat lignin.

DSC thermograms. Nevertheless, this technique was used to determine the T_g of PA 6 and of raw lignin. The samples were analyzed with their ambient moisture and were not previously dried. The PA6's T_g was observed at 18°C. As can be seen in Figure 2, in the case of lignin, the first heating thermogram is markedly disrupted by the presence of a broad endothermic peak covering and extending beyond its glassy region. This behavior has been explained by the highly amorphous nature of lignin with its complex hydrogen bonding interactions which can induce significant enthalpy relaxation.[53] In addition, as water evaporates also in this temperature range, this effect can be amplified by the presence of moisture. Dried lignin has been also analyzed by DSC (results not shown here) and results also showed the presence of this broad endothermic peak, meaning probably that trapped water remains in lignin. To overcome such strong enthalpy relaxation, the T_g of the native lignin, was determined from the second heating thermogram and was found to be about 140°C which indicates that lignin in the native state has strong intermolecular interactions.

While DSC is unsuccessful for blends T_g determination, it reveals a reduction of the crystallization (T_c) and melting temperatures (T_m) of the blends. T_c was measured from the cooling thermogram and T_m was determined from the second heating thermogram. As can be seen in Table II, the value of T_c decreases when the lignin increases. T_m tends to decrease with increasing lignin content but, as the melting temperature of PA6 is close to the decomposition temperature of the lignin, it was not possible to quantify the melting point suppression in this system. Crystallinity level (χ_c calculated per g of PA6 basis) remained unchanged with lignin content but similarly it can be impaired by the overlapping with lignin degradation. So, these values should be taken as estimations only. The change in T_c occurred probably because of lignin intermolecular interaction with PA6 through hydrogen bonds, which could be an indication of a significant evolution of the supermolecular structure mainly in terms of the PA6 crystal dimensions, thus hindering the formation of large crystalline structures. This result is consistent with the X-ray diffraction study conducted by Bittencourt *et al.* in which a reduction of the crystalline planes of PA6 was observed upon lignin addition.[54] A similar effect was observed for PEO/lignin system.[17,38,39]

Table II. DSC Measurements of PA6 and its Blends

Samples	T_c [°C]	T_m [°C]	χ_c [%]
PA6-L0	194	221	41
PA6-L5	192	220	41
PA6-L15	190	218	41
PA6-L30	187	217	42

In order to investigate more accurately the miscibility of PA6/lignin blends, DMA measurements were performed. DMA is a very sensitive technique and provides a valuable insight into the relationships between morphology, components interactions and mechanical properties of composite materials. The loss modulus (E'') and the loss factor (Tan δ) of neat lignin are presented in Figure 3. Neat lignin behaves like an amorphous polymer with a single transition attributed to the glassy region. The peak between 80°C and 120°C is assigned to water evaporation and the peak at 160°C measured from E'' is related to its T_g. The latter is higher than the one determined by DSC because of the difference in solicitations and equipment. The one measured by DSC is thermal T_g and do not exactly correspond to the dynamical T_g determined by DMA. These differences are well documented in literature.[55,56]

Figure 4 shows the temperature dependence in the glassy region of the storage modulus (E'), the loss factor (Tan δ) of neat PA6 in comparison with its blends with lignin. Overall, all the samples exhibit a relatively high storage modulus at low temperature and at room temperature indicating very rigid materials (Figure 4). For all samples, the storage modulus is about 4 GPa. Figure 4 also shows that the storage modulus slowly decreases with increasing temperature. The neat PA 6 shows a typical behavior of semi-crystalline polymer with three distinct regions that could be identified as the glassy, glass transition, and rubbery regions. In the glassy region, the storage modulus remains roughly constant. A deflection around 20°C is observed for PA6 which is related to the changes at its glass transition temperature (T_g); i.e. the temperature where the polymer chain segments start moving and change their state from glassy to rubbery. The glass transition temperature (T_g) is usually defined as the peak in the loss modulus (E'') versus temperature curves. T_g values for references and the blends are listed in Table III.

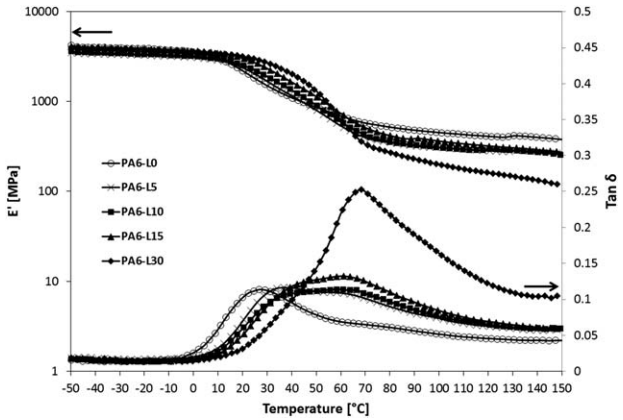

Figure 4. Storage Modulus (E') and Phase angle (Tan δ) of neat PA6 and its blends.

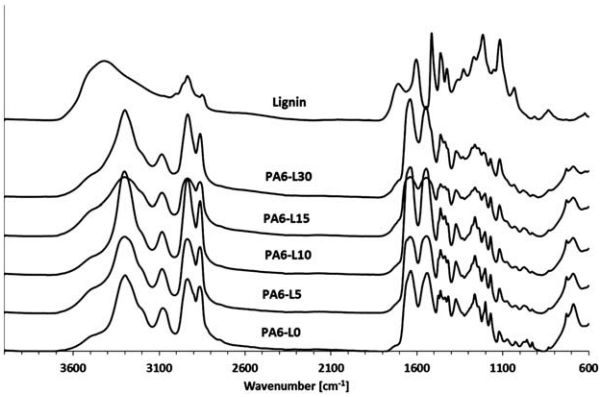

Figure 5. FTIR spectra of PA6/lignin blends in comparison with their parent polymer.

Adding lignin increases the T_g from 18°C for neat PA6 to 43°C for PA6-L30. The fact that single T_g was observed in the blends indicated the existence of a single-phase system with homogeneous miscibility at a dimensional scale of 5 and 15 nm and a high specific interaction system.[42,57,58] However, at higher temperature, the storage modulus (E') decreases with the lignin content, which can be interpreted as lower thermal stability of lignin/PA6 composites. This effect can be attributed to the competition between interaction improvement and the plasticizing effect of lignin. This behavior has been also observed during the blends processing where the extrusion torque was seen to decrease with addition of lignin and can confirm the storage moduli results at high temperature.

This observation is confirmed also by the loss factor (Tan δ) presented in Figure 4 where a broad peak, related to T_g, shifts to high temperature with increasing lignin content. This glass transition, broader than those of the constituent components, is usually observed in miscible polymer blends. This behavior is caused by the intrinsic difference between the local chain segment mobility of PA6 and lignin components. This observation confirms the morphological investigations by TEM indicating that PA6 and lignin are homogenous and miscible at 1–2 nm scale.

From the peak in the Tan δ curve, it can be seen also, that the incorporation of lignin affects significantly the glass transition temperature of the blend. This means that the overall chain mobility is very sensitive to the presence of lignin. Adding lignin increases the contribution of the viscous part to the dynamic response and decreases chain entanglement in the rubbery plateau region, which in turn decreases the thermal stability of the composites at higher temperature. The same phenomenon has been observed by Barzegari *et al.* when they added a compatibilizer in order to increase the interfacial adhesion between lignin and polystyrene.[47]

Table III. Glass Transition Temperature (T_g) of References and PA6/Lignin Blends Measured from the Loss Modulus (E'')

Samples	T_g (°C)
PA6-L0	18
PA6-L5	26
PA6-L10	29
PA6-L15	31
PA6-L30	43
Lignin	160

On the other hand, Figure 4 shows that the magnitude of Tan δ_{max} peak values increases with lignin amount, which is indicative of high degree of chain segment mobility in the amorphous region of PA6 brought about by the incorporation of lignin and good damping characteristics.

Structural Properties

The molecular interactions between lignin and PA6 were studied by infrared spectroscopy. Microscopic and DMA characterizations demonstrated that the blends under 30 wt % of lignin are miscible with homogeneous phase behavior. Specific molecular interactions can be expected to occur between the functional groups of lignin and PA6. FTIR is the most effective technique to investigate, in the solid state specific, intermolecular interactions between polymers and to understand the blends miscibility. If lignin intermolecularly interacted with another component in the blends, lignin or PA6 spectra in specific regions should exhibit differences because of the change of the chemical environment of their respective functional groups. FTIR investigations have been performed extensively on various naturally occurring lignins.[7,13,59] Because of the ether linkages, strong bands appear in the 1200–1000 cm^{-1} range. The IR vibrational bands rising from the aromatic rings and phenolic groups are detected between 1500 and 1200 cm^{-1}. The additional bands between 900–750 cm^{-1} are assigned to the substituents in the aromatic rings.

Figures 5 and 6 present the FTIR spectra for the PA6/lignin blends in comparison with their respective neat polymers. For clarity, all of the FTIR spectra shown here were shifted vertically. The spectra were normalized with respect to the 1168 cm^{-1} absorption band, which corresponds to the CH_2 twist/wag of PA6. To confirm that our observations are not biased by this normalization, a second normalization was done with the 2860 cm^{-1} absorption band. The same tendency in the

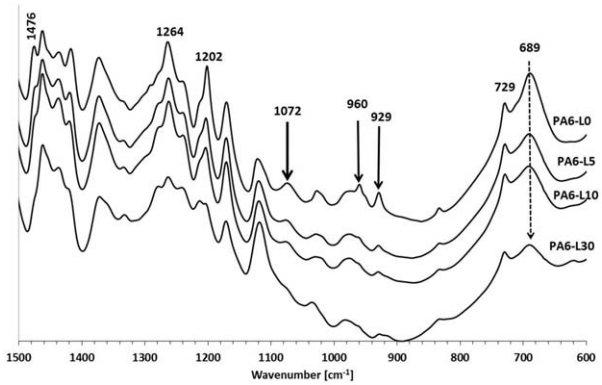

Figure 6. FTIR spectra of PA6/lignin blends in 600–1500 cm^{-1} region.

changes of the shape or height of the absorbance bands was observed.

Despite the strong overlapping of the parent spectra, a major difference can be observed in the 500–1500 cm^{-1} region of the PA6 spectrum which is attributed to its methylene sequence and crystalline forms (Figure 6). Upon addition of lignin, a decrease of the relative intensities of the PA6 bands at 1476 cm^{-1} (CH_2 wagging vibration), 1264 cm^{-1} (N-H bending and C-N stretching), 1202 cm^{-1} (CH_2 twist-wagging vibration), 1027 cm^{-1} (CH_2 wagging vibration), 960 and 930 cm^{-1} (CO-NH in plane vibration), 690 cm^{-1} [out of plane bending of N-H (amide V)] is observed likely indicating the presence of chain folding and phase changes in PA6. A conformational change in the PA6 chain could be attributed to the reactive intermolecular interaction between the two components. New specific hydrogen-bonding interactions formed between hydroxyl groups of lignin and amine groups of the PA6 can be postulated as the most likely to explain these changes. Similar interactions with lignin and others polymers have already been mentioned in literature for others blends.[17,18,34,36,38,39,42,49,51] These results corroborate all the previous TEM, TGA, and DMA results and based on all these analyses, the Scheme 1 can be proposed to show the probable interactions of lignin with PA 6.

Thermal Stability

TGA was performed to evaluate the degradation of lignin and to define the highest acceptable processing temperature of the blends. The thermal behavior of virgin lignin was studied by TGA under nitrogen and oxygen atmosphere. The TGA and DTGA curves are shown in Figure 7 for a constant heating rate of 10°C/min. Whatever the atmosphere condition, Figure 7

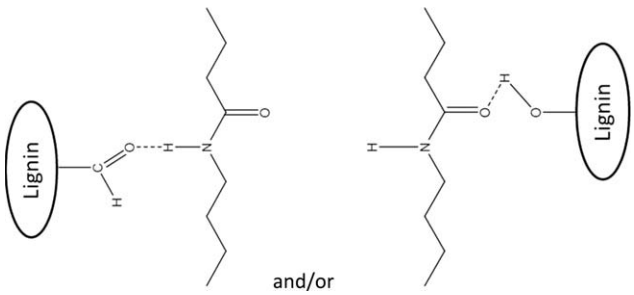

Scheme 1. Possible interactions sites of lignin with PA6

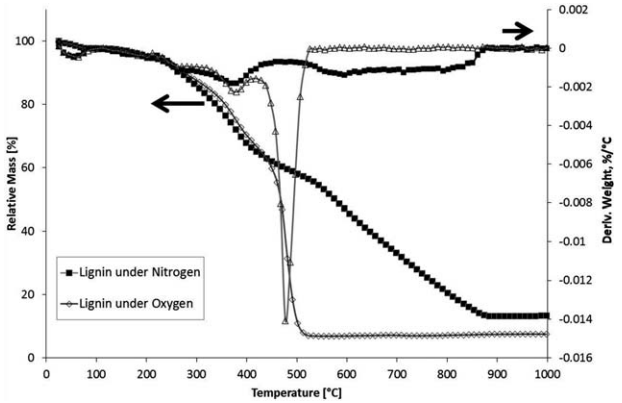

Figure 7. TGA curves under nitrogen and oxygen atmospheres of neat lignin.

reveals that lignin exhibits the same behavior up to 400°C: a first weight loss begins around 100°C, because of the presence of residual water, a second weight loss starts at about 200°C followed by a third weight loss exhibiting its highest rate (DTGA peak) at 370°C. This latter was mainly attributed to hemicellulose and cellulose pyrolysis.[4,60–62]

Beyond 400°C, the TGA and DTGA curves of lignin show great differences under air or nitrogen. In nitrogen, neat lignin's decomposition occurred progressively over the whole temperature range from 200°C to about 900°C and produces a high amount of char. There is still around 15% solid residues left even at 1000°C. In nitrogen, lignin can reasonably resist up to 650°C, while in air complete lignin degradation occurred below 500°C with a sharp peak at 477°C and a lower amount of char (<10 wt %).

Figure 8 presents the TGA curves of pristine PA6, neat lignin and their blends under nitrogen at a heating rate of 10°C/min and the inset table summarizes the respective onset decomposition temperatures (T10). The degradation temperature of neat PA6 and blends are different. Pristine PA6 exhibited single stage degradation with a peak at 500°C whereas the lignin blends show two degradation peaks in the range of 500–600°C. Figure 8 indicates that the onset temperature of rapid thermal degradation (T10) decreases with increasing lignin loading. By adding lignin, the thermal degradation (T10) of the blends decreased, and the degradation is completed around 600°C. The results also show that the thermal stability of the blends decreased as the lignin content increased because of the lower thermal stability of lignin compared to neat PA6. Also, this behavior could be assigned to the intermolecular interactions occurring between PA6 and lignin.[34] As a result, the blends produce no char residue. As can be seen from Figure 8, there is no solid residues at 1000°C. This can be explained by a blowing up of the blends giving form to a foam as the temperature increases steadily. This generated volatile char is gradually ejected from the crucibles by nitrogen flow sweeping. The blends char amount can be measured at around 600°C where the samples were still entirely in the crucibles. At this temperature, the char amount is about 4% for neat PA6 and PA-L5, 6% for PA-L10 and PA-L15, and around 10% for PA-L30.

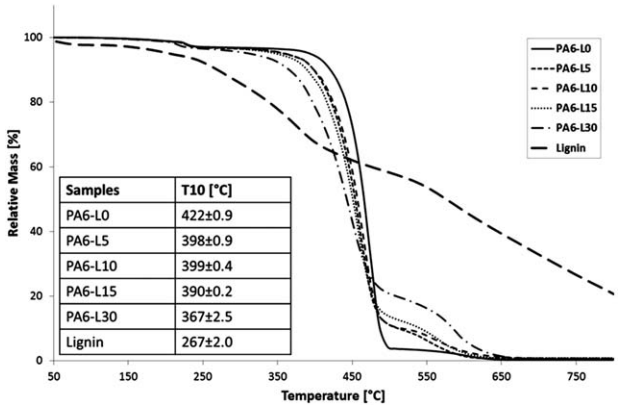

Figure 8. TGA curves under nitrogen atmosphere of neat PA6 and its blends.

Mechanical Properties

Figure 9 shows the representative stress–strain curves of neat PA6 and the different blends. All blends display a typical tensile behavior of semi-crystalline polymers characterized by an initial elastic region followed by the appearance of a neck (i.e. yield point) and undergo plastic deformation. Within this neck, the chains become aligned parallel to the elongation direction, leading to strain hardening. The neck propagates along the gauge length until failure occurs. Interestingly, as the lignin amount increases, stress decreases while strain at break is maintained. Figure 10 and Table IV summarize the tensile properties for neat PA6 and its blends. With lignin addition, all the mechanical properties are maintained. Young's modulus slightly increases with lignin addition (Figure 10), it is around 800 MPa for neat PA6 and about 840 MPa for its blends. Whatever lignin fraction, the Yield stress is about 41 MPa. Also, the elongation at break is preserved and slightly improved with lignin addition. It can be seen from Figure 9 and Table IV that the elongation at break is closer to the one of neat PA6 although the stress values are lower, confirming the surprising ease of hand stretching of the extruded strands. This improvement in ductility with lignin addition can be attributed to both lignin plasticization effect and miscible blending between PA6 and lignin. Such a behavior has already been observed for partially miscible blend of polyvinylidene fluoride and polytetramethylene adipate.[63] According to the authors small concentrations of polyester

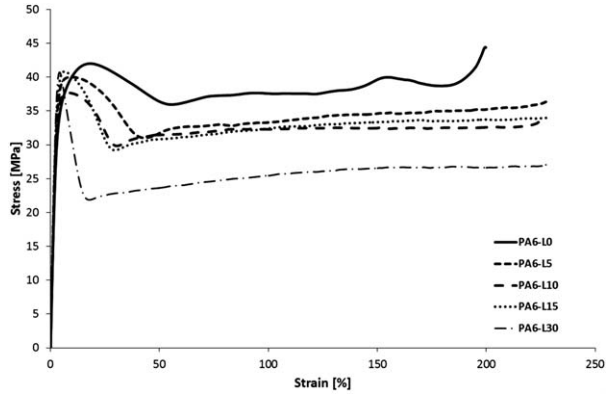

Figure 9. Mechanical behavior of PA6/lignin blends by uniaxial stretching.

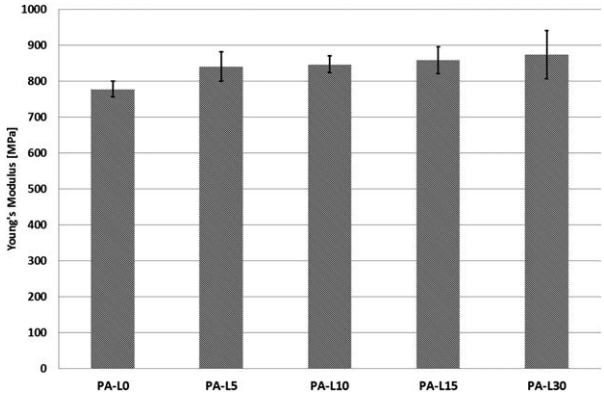

Figure 10. Young's modulus of PA6/lignin blends.

modify the lamellar microstructure and act as a plasticizer. Sailaja *et al.* have demonstrated the same effect in a compatibilized composite of polyethylene and modified lignin via an esterified route.[32] They attributed the elongation improvement to an internal plasticization of the esters functionalities owing to improved compatibilization of polyethylene and lignin. The mechanical properties of these alloys show similar trends as ones examined in this study.

CONCLUSIONS

In conclusion, technical lignin and PA6 blends were prepared via twin screw extrusion process and were found to be miscible as deduced from structural and thermal investigations showing homogeneous blends. PA6/lignin miscibility has been observed for lignin amount up to 30 wt %. The T_g is shifted to high temperature upon blending indicating strong intermolecular interactions. FTIR further revealed the presence of strong hydrogen bonding between the two polymers in the blends as shifts in IR frequencies clearly suggested. The basis for the miscibility in the lignin/PA6 blends is most likely hydrogen-bonding interactions between the hydroxyl hydrogen of lignin and the hydrogen acceptor sites of PA6. Overall, mechanical properties have been found to be close to the PA6's ones, in terms of Young modulus and yield stress. Although the stress decreases with the addition of lignin, interestingly the elongation at break was not affected. On the contrary, the addition of lignin seems to lead to an enhancement of the blends ductility. This behavior can be attributed to a plasticization effect of lignin and to the strong hydrogen-bonding interactions formed between hydroxyl groups of lignin and amine groups of the PA6.

Table IV. Mechanical Properties of PA6/Lignin Blends

Samples	Yield stress [MPa]	Elongation at break [%]
PA6-L0	41.6 ± 2	208 ± 11
PA6-L5	38.7 ± 1	227
PA6-L10	39 ± 2	226 ± 1
PA6-L15	41 ± 1	227
PA6-L30	41 ± 4	227

ACKNOWLEDGMENTS

The authors acknowledge the support from Walloon Region (DEXPLIMAR project no. 6758).

REFERENCES

1. Ragauskas, A. J.; Williams, C. K.; Davison, B. H.; Britovsek, G.; Cairney, J.; Eckert, C. A.; Frederick, W. J.; Hallett, J. P.; Leak, D. J.; Liotta, C. L.; Mielenz, J. R.; Murphy, R.; Templer, R.; Tschaplinski, T. *Science* **2006**, *311*, 484.
2. Bidgwater, A. V. *Therm. Sci.* **2004**, *8*, 21.
3. Holladay, J. E; Bozell, J. J.; White, J. F.; Johnson, D. Report available via: http://www1.eere.energy.gov/biomass/pdfs/pnnl-16983.pdf **2007**, 1.
4. Brebu, M.; Vasile, C. *Cell. Chem. Technol.* **2010**, *44*, 353.
5. Kamm, B.; Kamm, M. *Appl. Microbiol. Biotechnol.* **2004**, *64*, 137.
6. Delmas, M. *Chem. Eng. Technol.* **2008**, *31*, 792.
7. Sahoo, S.; Seydibeyoglu, M.; Mohanty, A. K.; Misra, M. *Biomass Bioenergy* **2011**, *35*, 4230.
8. Agrawal, A.; Kaushik, N.; Biswas, S. *Scitech J.* **2014**, *01*, 30.
9. Gargulak, J. D.; Lebo, S. E. In Lignin: Historical, Biological and Materials Perspectives; Glasser, W. G.; Northey, R. A.; Schultz, T. P., Eds.; ACS Symposium Series, **2000;** Vol. *742*, Chapter 15, p 304.
10. Crestini, C.; Melone, F.; Sette, M.; Saladino, R. *Biomacromolecules* **2011**, *12*, 3362.
11. Sette, M.; Wechselberger, R.; Crestini, C. *Chem. Eur. J.* **2011**, *17*, 9529.
12. Higuchi, T. *Wood Sci. Technol.* **1990**, *24*, 23.
13. Kubo, S.; Kadla, J. F. *Biomacromolecules* **2005**, *6*, 2815.
14. Laurichesse, S.; Avérous, L. *Prog. Polym. Sci.* **2014**, *39*, 1266.
15. Adler, E. *Wood Sci. Technol.* **1977**, *11*, 169.
16. Kadla, J. F.; Kubo, S.; Venditti, R. A.; Gilbert, R. D.; Compere, A. L.; Griffith, C. W. *Carbon* **2002**, *40*, 2913.
17. Kadla, J. F.; Kubo, S. *Macromolecules* **2003**, *36*, 7803.
18. Kubo, S.; Kadla, J. F. *J. Polym. Environ.* **2005**, *13*, 97.
19. Brodin, I.; Ernstsson, M.; Gellerstedt, G.; Sjöholm, E. *Holzforschung* **2012**, *66*, 141.
20. Thunga, M.; Chen, K.; Grewell, D.; Kessler, M. R. *Carbon* **2014**, *68*, 159.
21. Ramasubramanian, G. Graduate Theses and Dissertations, **2013**, Paper 13438.
22. Fernandes, E. M.; Aroso, I. M.; Mano, J. F.; Covas, J. A.; Reis, R. L. *Compos. Part B Eng.* **2014**, *67*, 371.
23. Xu, G.; Yan, G.; Zhang, J. *Polym. Bull.* **2015**, 1.
24. Košíková, B.; Gregorová, A.; Osvald, A.; Krajcŏvicŏva, J. *J. Appl. Polym. Sci.* **2007**, *103*, 1226.
25. Pouteau, C.; Dole, P.; Cathala, B.; Averous, L.; Boquillon, N. *Polym. Degrad. Stab.* **2003**, *81*, 9.
26. Dawson, B. S. W.; Singh, A. P.; Kroese, H. W.; Schwitzer, M. A.; Gallagher, S.; Riddiough, S. J.; Wu, S. H. *J. Coat. Technol. Res.* **2008**, *5*, 193.
27. Ismail, T.; Abu Hassan, H.; Hirose, S.; Taguchi, Y.; Hatakeyama, T.; Hatakeyama, H. *Polym. Int.* **2010**, *59*, 181.
28. Li, J.; He, Y.; Inoue, Y. *Polym. Int.* **2003**, *52*, 949.
29. Canetti, M.; Bertini, F.; De Chirico, A.; Audisio, G. *Polym. Degrad. Stab.* **2006**, *91*, 494.
30. Saito, T.; Brown, R. H.; Hunt, M. A.; Pickel, D. L.; Pickel, J. M.; Messman, J. M.; Baker, F. S.; Keller, M. A.; Naskar, K. *Green Chem.* **2012**, *14*, 3295.
31. Alexy, P.; Košíková, B.; Podstránska, G. *Polymer* **2000**, *41*, 4901.
32. Sailaja, R. R. N.; Deepthi, M. V. *Mater. Des.* **2010**, *31*, 4369.
33. Sadeghifar, H.; Cui, C.; Argyropoulos, D. S. *Ind. Eng. Chem. Res.* **2012**, *51*, 16713.
34. Canetti, M.; Bertini, F. *ePolym.* **2009**, 049.
35. Canetti, M.; Bertini, F. *Compos. Sci. Technol.* **2007**, *67*, 3151.
36. Kadla, J. F.; Kubo, S. *Compos. Part A* **2004**, *35*, 395.
37. Corradini, E.; Pineda, E. A. G.; Hechenleitner, A. A. W. *Polym. Degrad. Stab.* **1999**, *66*, 199.
38. Kubo, S.; Kadla, J. F. *Macromolecules* **2004**, *37*, 6904.
39. Kubo, S.; Kadla, J. F. *J. Appl. Polym. Sci.* **2005**, *98*, 1437.
40. Feldman, D.; Banu, D.; Campanelli, J.; Zhu, H. *J. Appl. Polym. Sci.* **2001**, *81*, 861.
41. Pouteau, C.; Baumberger, S.; Cathala, B.; Dole, P. *C. R. Biol.* **2004**, *327*, 935.
42. Mishra, S. B.; Mishra, A. K.; Kaushik, N. K.; Khan, M. A. *J. Mater. Process. Technol.* **2007**, *183*, 273.
43. De Chirico, A.; Armanini, M.; Chini, P.; Cioccolo, G.; Provasoli, F.; Audisio, G. *Polym. Degrad. Stab.* **2003**, *79*, 139.
44. Zhong, M.; Dai, H.; Yao, H.; Da, D.; Zhou, Y.; Yang, J.; Chen, F. *SPE* **2011**, 1. 10.1002/spepro.003642
45. Chen, F.; Dai, H.; Dong, X.; Yang, J.; Zhong, M. *Polym. Compos.* **2011**, 1019.
46. Samal, S. K.; Fernandes, E. G.; Corti, A.; Chiellini, E. *J. Polym. Environ.* **2014**, *22*, 58.
47. Barzegari, M. R.; Alemdar, A.; Zhang, Y.; Rodrigue, D. *Polym. Polym. Compos.* **2013**, *21*, 357.
48. Nitz, H.; Semke, H.; Mülhaupt, R. *Macromol. Mater. Eng.* **2001**, *286*, 737.
49. Mousavioun, P.; Doherty, W. O. S.; George, G. *Ind. Crops Prod.* **2010**, *32*, 656.
50. Rahman, M. A.; De Santis, D.; Spagnoli, G.; Ramorino, G.; Penco, M.; Phuong, V. T.; Lazzeri, A. *J. Appl. Polym. Sci.* **2013**, 202. DOI: 10.1002/APP.38705
51. Teramoto, Y.; Lee, S. H.; Endo, T. *J. Appl. Polym. Sci.* **2012**, *125*, 2063.
52. Carlier, V.; Sclavons, M.; Legras, R. *Polymer* **2001**, *42*, 5327.
53. Cui, C.; Sadeghifar, H.; Sen, S.; Argyropoulos, D. S. *Bioresources* **2013**, *8*, 864.
54. Bittencourt, P. R. S.; Fernandes, D. M.; Silva, M. F.; Lima, M. K.; Hechenleitner, A. A. W.; Pineda, E. A. G. *Waste Biomass Valor* **2010**, *1*, 323.
55. Schawe, J. E. K. *J. Polym. Sci. Part B: Polym. Phys.* **1998**, *36*, 2165.

56. Schawe, J. E. K. Elastomers Collected Applications Thermal Analysis, Eds.; Mettler Toledo, **2002**; Vol. *1*, p 35.
57. Woo, E. M.; Wu, M. N. *Polymer* **1996**, *37*, 1907.
58. Paul, D. R.; Bucknall, C. B., Eds.; In Polymer Blends: Formulation and Performance; John Wiley & Sons: New York, **2000**, Vol. *1*, p 539.
59. Derkacheva, O.; Sukhov, D. *Macromol. Symp.* **2008**, *265*, 61.
60. Yang, H.; Yan, R.; Chen, H.; Lee, D. H.; Zheng, C. *Fuel* **2007**, *86*, 1781.
61. Vanderghem, C.; Richel, A.; Jacquet, N.; Blecker, C.; Paquot, M. *Polym. Degrad. Stab.* **2011**, *96*, 1761.
62. Wu, Y. M.; Zhao, Z. L.; Li, H. B.; He, F. *J. Fuel Chem. Technol.* **2009**, *37*, 427.
63. Reckinger, C.; Rault, J. *Revue Phys. Appl.* **1986**, *21*, 11.